REE and Neodymium isotope distribution in the northern South China Sea: particulate dissolution versus water mass mixing

Qiong Wu[1*], Zhifei Liu[2], Christophe Colin[3], Eric Douville[4], Yulong Zhao[2], Arnaud Dapoigny[4], Louise Bordier[4], Yi Huang[3], Pengfei Ma[2]

1. College of Oceanography, Hohai University, 210098 Nanjing, China

2. State Key Laboratory of Marine Geology, Tongji University, Shanghai 200092, China.

3. Université Paris-Saclay, CNRS, GEOPS, 91405, Orsay, France.

4. Laboratoire des Sciences du Climat et de l'Environnement, LSCE/IPSL, CEA-CNRS-UVSQ, Université Paris-Saclay, 91191 Gif-sur-Yvette, France.

Corresponding author: Qiong Wu (qiongwu@hhu.edu.cn)

Key points :

1. Rare earth elements concentrations and Nd isotopes of surface seawater in the South China Sea are influenced by local terrigenous inputs

2. Seasonal variations of rare earth elements fractionation is related to lateral mixing of water masses induced by regional monsoon activities

3. Nd values of deep water are similar to that of the West Pacific suggesting the fed of Pacific Deep Water to the deep South China Sea

Abstract

Dissolved rare earth elements (REE) and neodymium isotopic compositions (Nd) were intensively used to evaluate water mass mixing and lithogenic inputs in oceans. The South China Sea (SCS) is the largest marginal sea and a key region for reconstructing past hydrological changes in the West Pacific; however, its REE and Nd distribution are still not well established. This study investigated dissolved REE concentration and Nd distribution at four water stations in the northern and central SCS to better constrain the Nd distribution and REE cycle in the SCS. The results show relatively high concentrations of REE in surface seawater due to the terrigenous inputs. Seasonal variability in the middle REE enrichment is observed, suggesting a controlling role of the lateral mixing of water masses in the REE fractionation. The decreased REE concentrations in bottom water are mainly attributed to the re-suspended particle scavenging. Surface seawater Nd varies from -2.8±0.3 to -6.7±0.3, implying a significant modification due to riverine inputs. The intermediate water is characterized by a slightly negative Nd compared to the North Pacific Intermediate Water (NPIW) suggesting a vertical mixing between the intermediate and deep water within the SCS. Nd of deep water shows a narrow range from -3.4±0.3 to -4.2±0.3 (mean value of ~-3.8), supporting the presence of Pacific Deep Water (PDW) in the deep SCS basins nowadays. Nd of deep water in the SCS behaves conservatively along its pathway from the West Pacific to the SCS even though particle scavenging occurs in bottom water.

Plain language summary

Newly determined dissolved rare earth elements (REE) concentrations and neodymium isotope (Nd) distributions are presented for the South China Sea (SCS) to study water mass mixing and regional terrigenous inputs. Dissolved REE results from the northern and central SCS show that inputs arising from continental weathering have a considerable impact on REE distribution in SCS surface waters. The vertical distributions of middle REE are characterized by seasonal variability indicating mixing of laterally transported water masses associated with seasonally reversed monsoon activities. Significant variability in surface seawater Nd in the SCS is interpreted as being a result of particulate dissolution induced by large scale sediment discharge from surrounding Asian rivers. Due to intensive vertical mixing of deep water with intermediate water in the SCS, Nd values of intermediate water are relatively more negative than those of North Pacific Intermediate Water (NPIW). The deep water Nd values show a narrow range, from -3.4±0.3 to -4.2±0.3, in agreement with the presence of Pacific Deep Water (PDW) in the deep SCS basins. Nd of deep water in the SCS behaves conservatively along its pathway from the West Pacific to the central SCS despite the fact that particle scavenging occurs in bottom water.

1. Introduction

Dissolved Nd isotopes have been intensively used over the last decade to track past changes in ocean circulation at different times scales (Piotrowski et al., 2012; Scher et al., 2015; Molina-Kescher et al., 2016; van de Flierdt e al., 2016; Tachikawa et al., 2017; Colin et al., 2021). The vertical profiles of rare earth elements (REE) concentrations are similar to those of nutrients, with deep waters being typically more enriched in REE than upper layer waters (Elderfield., 1988; Alibo and Nozaki., 2003; de barr et al., 2018). This suggests that REE take part in vertical biogeochemical cycling and that the siliceous matter takes up REE from the surface and later releases REE to seawater as it settles downward (Akagi., 2013; Garcia-Solsona et al., 2014). In addition to lateral transport by water masses, riverine and dust inputs and "boundary exchange" can also contribute to modified dissolved REE concentrations and patterns in the ocean (Rousseau et al., 2015; Stichel et al., 2015; Yu et al., 2017). Several studies show that the relative enrichment of middle REE (MREE) and less depleted Ce for surface seawater are most likely linked to inputs of external sources (Greaves et al., 1994; Grasse et al., 2017, Yu et al., 2017; Hathorne et al., 2020). Some studies also suggest that submarine groundwater discharge could be a significant contributor to the REE budget of coastal seawater (Johannesson and Burdige., 2007; Kim and Kim., 2014). In addition, it has been suggested that the diffusive benthic flux of REE from pore fluid to bottom water potentially compensates for the "missing" flux of REE in the ocean which is predicted by modeling (Abbott et al., 2015; Haley et al., 2017).

The distribution of dissolved Nd concentration and its isotopic composition are extensively used to better understand the Nd and more generally REE cycles in the ocean (van de Flierdt et al., 2016 and references therein; Tachikawa

et al., 2017). The Nd isotopic composition ($^{143}Nd/^{144}Nd$, expressed as Nd) of seawater is usually considered as a quasi-conservative proxy to track water mass provenance and is widely applied in paleoceanography and paleo-environmental studies at various time scales (Piotrowski et al., 2005; Scher et al., 2015; Dubois-Dauphin et al., 2016; Le Houedec et al., 2016; Tachikawa et al., 2017; Colin et al., 2019, 2021; Wu et al., 2019; Du et al., 2020 and references therein). Nevertheless, recent studies reveal that seawater-derived Nd extracted from authigenic phases is not completely reliable for reconstructing past ocean circulation in certain regions (Osborne et al., 2014; Abbott et al., 2015; Tachikawa et al., 2017). The main debate on the reliability of Nd as a paleo-seawater tracer centers on whether the record of temporal seawater Nd signature can faithfully reflect water mass mixing (Tachikawa et al., 2017; Du et al., 2020).

The input of continental REE to the ocean was found to significantly modify current seawater Nd signature, especially for surface water, through the addition and/or removal of Nd by a particle-seawater exchange process (Lacan and Jeandel., 2005; Sighn et al., 2012; Yu et al., 2017). It has been suggested that the boundary exchange or lithogenic input during the period with lower sea level may also have produced a shift in the temporal seawater Nd value to sediment Nd value in the past (Nobel et al., 2013; Wu et al., 2017). In addition, whether the sedimentary archived Nd values could have been altered due to the variability of redox conditions is also debated (Du et al., 2016; Haley et al., 2017). Studies on Nd isotopes extracted from sedimentary coatings illustrate that Nd released from pore fluid can modify the original seawater Nd signature that was incorporated into authigenic phases at the sediment-seawater interface. In addition, Nd released from pore fluid can be also a benthic source to bottom water, leading to the alteration of the primary seawater Nd value (Abbott et al., 2016; Du et al., 2016). Consequently, the processes could potentially influence the conservative behavior of seawater Nd isotopes. The reliability of the application of seawater derived Nd isotopes in paleoceanographic studies therefore requires further investigation, especially on the various marginal seas affected largely by terrigenous detrital inputs.

The South China Sea (SCS) is the largest marginal sea in the western Pacific Ocean and is surrounded by numerous large Asian rivers that are characterized by substantial sediment discharges (Milliman and Farnsworth, 2011; Figure 1). In this case, the SCS is an important area to study the processes controlling the REE and Nd cycling. In addition, a better understanding of seawater REE and Nd distributions in the SCS could provide clues on the present-day circulation of the West Pacific, which in turn corroborate the the use of Nd as a proxy to track water masses in the geological past. Several studies have indicated a decreasing gradient of Nd of surface water from the northern to the southern SCS whereas the maximum of Nd concentration occurs in the central gyre (Amakawa et al., 2000; Alibo and Nozaki., 2000; Wu et al., 2015). This indicates that in addition to lateral water mass mixing, there might be inputs of REE from local sources within the sea (Amakawa et al., 2000). The vertical profiles of dissolved REE and Nd are mainly confined to the northern SCS. To

date, little is known about the geochemical cycling of seawater REE and Nd within the central SCS (Amakawa et al., 2000; Alibo and Nozaki., 2000; Wu et al., 2015).

In this study, we investigated the vertical profiles of dissolved REE concentration and Nd at four water stations in the northern and central SCS including four intermediate-bottom water samples obtained from station around drift sediment near Dongsha Island. Our aims are (1) to better constrain the sources and geochemical cycling of dissolved REE within the SCS, (2) to better understand the relative contribution of mixing processes and external lithogenic input on the distribution of regional dissolved REE and Nd. We aim to evaluate processes that might have a potential influence on the conservative behavior of Nd as it is transported from the West Pacific to the central SCS.

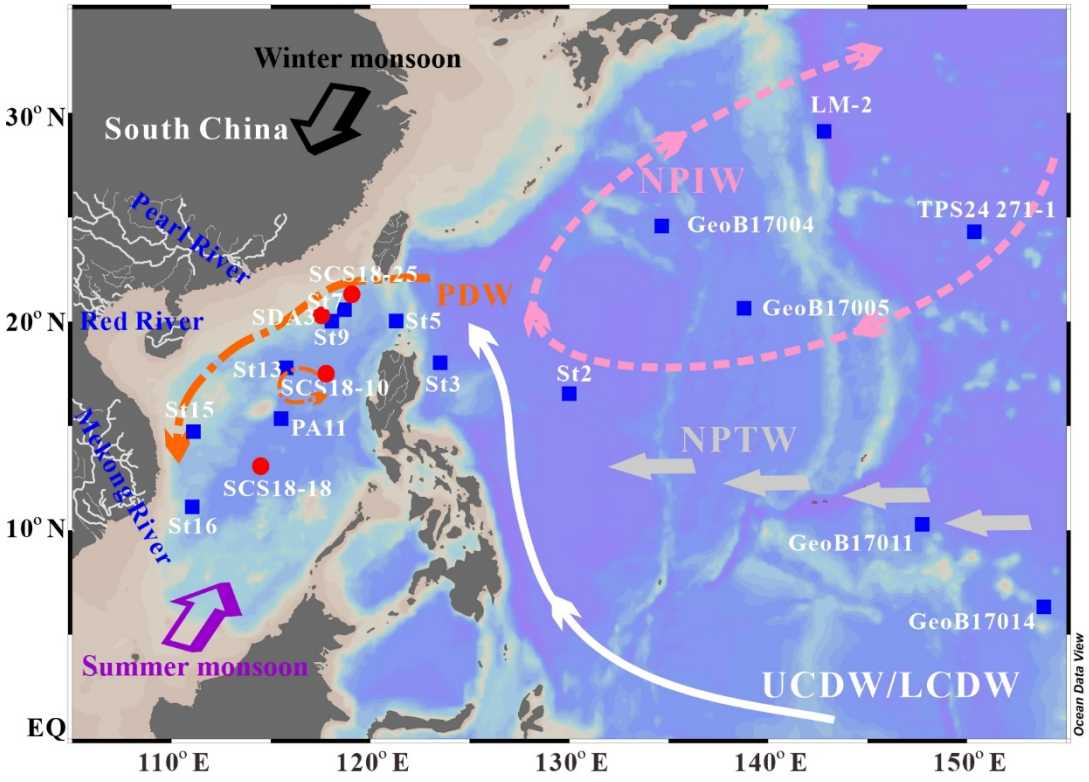

Figure 1. Sampling map showing seawater stations mentioned in text and regional oceanic current pattern. The red dots represent sampling stations in this study, while blue squares show published stations discussed in the text (Piegras and Jacobsen., 1988; Amakawa et al., 2004; Wu et al., 2015; Brehens et al., 2018a). The white line denotes schematic pathway of the Upper/Lower Circumpolar Deep Water (UCDW/LCDW) in the western Pacific Ocean (modified after Kawabe and Fujo., 2010). The flow path of North Pacific Intermediate

Water (NPIW) is indicated by pink dashed line (after You, 2003). The North Pacific Tropical water is shown in gray arrows. The flow direction of Pacific Deep Water (PDW) in the South China Sea is shown by orange dashed lines. The local seasonal reversed monsoon directions are indicated by black and purple arrows. The map was produced using Ocean Data View (ODV) (Schlitzer, 2014).

2. Regional oceanography

The SCS is a semi-enclosed marginal sea connecting the Pacific Ocean and the Indian Ocean. It is connected to the western Pacific Ocean through a single deep channel, the Luzon Strait. Previous studies have revealed a well-recognized vertical sandwich structure made up of three layers of inflow-outflow-inflow in the upper, intermediate and deep layers respectively across the Luzon Strait (Yuan et al., 2002; Tian et al.,2006; Shu et al., 2014; Gan et al., 2016; Zhu et al., 2016, 2019; Wang et al., 2019). The surface circulation of the SCS is mainly driven by a complex system including seasonally reversed monsoon activity, tidal processes and other dynamic processes (Fang et al., 1998; Li and Qu., 2006; Zhang et al., 2018; Wang et al., 2019). In general, the surface circulation in the southern SCS is basically driven by the seasonal reversal of monsoon winds that induce cyclonic gyre during the winter and anti-cyclonic gyre during the summer (Fang et al., 1998). In the northern SCS, the forcing of reversal monsoon winds and the intrusion of the Kuroshio branch makes the surface currents more complex (Fang et al., 1998; Wang et al., 2013). Apart from the wind-driven gyres, mesoscale anti-cyclonic eddies and coastal currents exist in the area of the northern continental slope (Hu et al., 2000; Yuan et al., 2006; Wang et al., 2021).

The intermediate water, characterized by relatively low salinity, plays an important role in the formation of meridional overturning circulation in the SCS (Tian et al., 2006; Yang et al., 2010; Gan et al., 2016; Zhu et al., 2016; Wang et al., 2019; Figure 2). Previous studies have suggested that the net transport of intermediate water is from the SCS to the western Pacific Ocean, compensated by a net inflow of the upper- and deep-water masses (Tian et al., 2006., 2009). In addition, it has been demonstrated that the outflow of intermediate water occurs in the northern/southern part of the Luzon Strait in winter/summer while the temporal westward flow of intermediate water to the SCS occurs on the southern/northern part of the Luzon Strait (Tian et al., 2006; Yang et al., 2010; Zhu et al., 2016).

The deep water of the SCS is mainly fed by the PDW which itself originates from Upper/Lower Circumpolar Water. With the deepest sill at about 2400 m in the Luzon Strait, the physical property of deep water is relatively homogenous and is similar to PDW in the Philippine Sea at about 2000 m (Broecker et al., 1986; Qu et al., 2006; Zhu et al., 2019). A basin scale cyclonic deep current driven by the Luzon deep water overflow has been observed based on density and oxygen distribution, and further supported by model results (Qu et al., 2006; Gan et al., 2016; Zhu et al., 2017). The deep western boundary current along the northern

slope and the sub-basin scale recirculation current have also been identified through modeling and mooring observations (Wang et al., 2011; Zhou et al., 2017, 2020; Figure 1). In addition to these large-scale currents, mesoscale eddy dissipation has been suggested to force the horizontal circulation and vertical diffusion in the mid-deep layers, resulting in enhanced mid-deep mixing and ascension of deep water (Tian et al., 2009; Chen et al., 2015; Zhang et al., 2016).

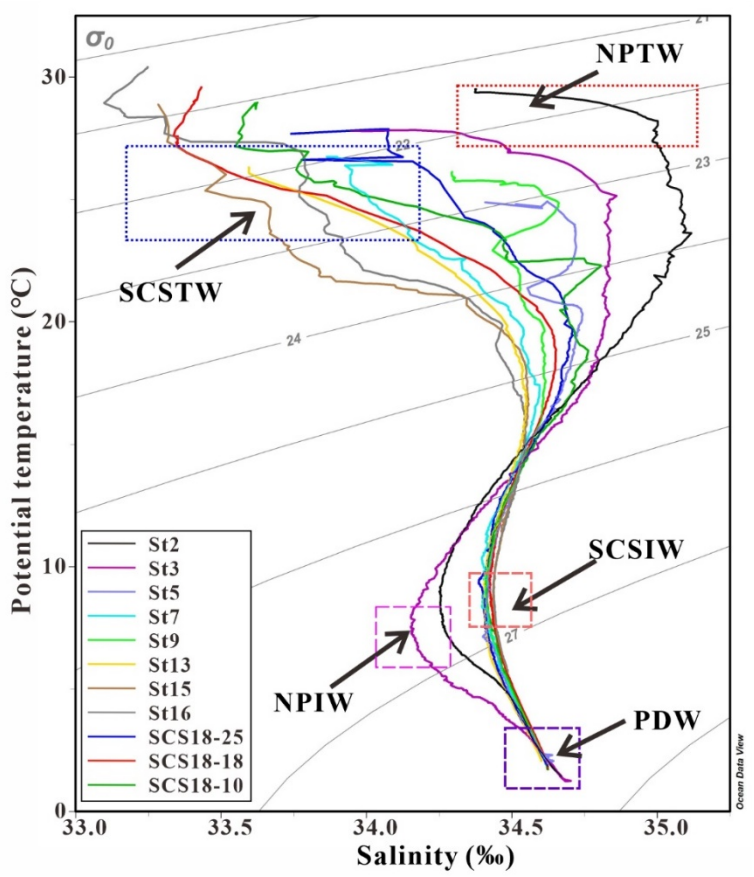

Figure 2. Physical water properties of sampled stations in this study and Wu et al., (2015). The water masses (North Pacific Tropical Water, South China Sea Tropical Water, North Pacific Intermediate Water, South China Sea Intermediate Water and Pacific Deep Water) in the western Pacific Ocean and the SCS are identified.

3. Materials and methods

In total, 56 seawater samples from four water stations were collected from the SCS during the KK1803 cruise carried out by R/V Jiageng from April to May 2018 (Figure 1). The northernmost water station, SCS18-25, is located on

the deep-water pathway after it crosses the Luzon Strait. Station SCS18-18, located in the central SCS basin is, to date, the southernmost station in the SCS with a vertical profile of seawater sampling. Station SCS18-10 is located in the northeastern SCS, between stations SCS18-25 and SCS18-18. Four seawater samples were collected from station SDA3, which is located in the north close to Dongsha island where a series of large sediment drifts has been identified (Lüdmann et al., 2005).

For the three water stations SCS18-10, SCS18-18 and SCS18-25, 10 L seawater sample was collected on board using Niskin bottles mounted on a 24-position Sea-Bird's 911plus CTD-rosette. Four additional intermediate-bottom water samples from station SDA3 were collected using 6 L Niskin bottles mounted on a ROV (ROPOS). About 500 ml seawater was subsampled onboard for REE concentration measurements. All seawater samples were immediately acidified to pH 2 with ultra-clean 6 N HCl after they had been filtered onboard. Back at the land-based laboratory, the seawater samples were treated following the protocol described by Copard et al. (2010).

In brief, the seawater was first pre-concentrated on a C^{18} SepPak cartridge. REE were separated from the matrix using Biorad AG50W-X8 (200-400 m mesh-size resin). Nd was then purified using Eichrom Ln-Spec resin (100-150 m mesh-size), following the procedure described in Copard et al. (2010). Nd isotopes of the purified fractions were measured on a ThermoScientific Neptune^{plus} Multi-Collector Inductively Coupled Plasma Mass Spectrometer (MC-ICP-MS) at the Laboratoire des Sciences du Climat et de l'Environnement (LSCE) in Gif-sur-Yvette (France). During the analytical sessions, every group of two samples was bracketed with analyses of appropriate Nd standard solution JNdi-1 ($^{143}Nd/^{144}Nd$ of 0.512115±0.000006; Tanaka et al., 2000). Sample and standard concentrations were matched at similar concentration of 10 ppb. The $^{143}Nd/^{144}Nd$ ratios were corrected for mass-dependent fractionation using $^{146}Nd/^{144}Nd = 0.7219$ and an exponential law. The offset value between the results and the certified values of JNdi-1 was less than 0.4 epsilon units for all of the analyses presented in this study. The analytical errors reported herein correspond to the external two-sigma standard deviation (based on repeated analyses of the JNdi-1 for the different analytical sessions). The analytical errors obtained ranged from 0.3 to 0.4 epsilon units. Procedural blanks corresponding to all analytical procedures, including the preconcentration of Nd from the seawater matrix, were < 200 pg which represents $< 1.6\%$ of the lowest Nd concentration of surface seawater in this study. As a result, no blank correction was applied.

Dissolved REE concentrations were measured on 250 ml seawater samples using the ThermoScientific XseriesII Inductively Coupled Plasma-mass Spectrometer (ICP-MS) at the LSCE following the procedure described by Wu et al. (2015). Briefly each sample was spiked with a Pr and Tm solution to correct the recovery of the REE after the complete chemical extraction procedures. REE were co-precipitated with ultra-pure iron hydroxide and then extracted by successive

ion exchange procedures (AG1W-X8 resin). REE concentrations were corrected of any sensitivity drift of the machine using In and Re as internal standards. Due to the systematic impact of the Pr spike on Tb, Tb concentrations are characterized by high uncertainty. The analytical uncertainties of our measurements are ranging from ~5% for the lightest REE, to ~15% for the heaviest REE. The total blank of REE averaged ~15% except for HREE Yb and Lu (averaged ~36% and ~40%) and was subtracted for all seawater samples.

4.Results

4.1 Physical water properties at studied stations

The potential temperature and salinity profiles of investigated stations in this study and several previous stations from Wu et al. (2015) are reported in Figures 2 and 3. According to these physical water properties, water masses identified in stations SCS18-10, SCS18-18 and SCS18-25 can be defined as SCSTW, SCSIW and PDW. Figure 2 indicates that the hydrographic parameters of water masses in the SCS are distinguishable from the western Pacific for the surface and intermediate layers. This result is similar to those reported in previous studies (Tian et al., 2009; Wu et al., 2015). The salinity maximum mainly occurs at about 150 m in the SCS and is relatively low compared to its counterpart NPTW in the Philippine Sea.

For the intermediate layer, the SCS intermediate water (SCSIW) is characterized by a salinity minimum of ~34.38 between 300 m and 500 m (Figures 2 and 3). In addition, due to vertical diffusion from the deep layer, the salinity minimum of SCSIW is slightly higher than that of North Pacific Intermediate Water (NPIW) at stations in the Philippine Sea (Figure 2, Wu et al., 2015). Below 2000 m, the water masses in the SCS are characterized by an almost constant salinity of ~34.6.

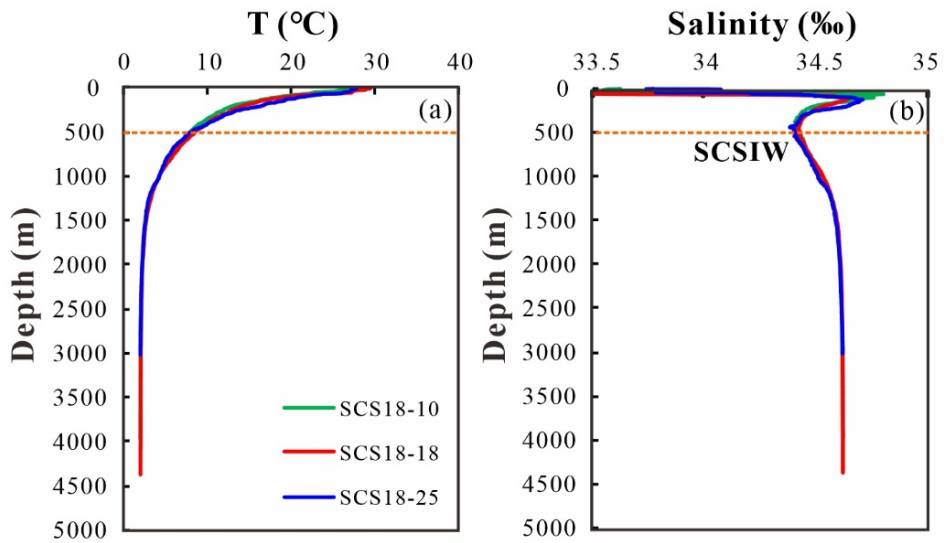

Figure 3. Depth profiles of potential temperature (a) and salinity (b) at three stations of this study. The salinity minimum of intermediate water occurs at about 500 m.

4.2 Seawater Nd isotopes

Dissolved Nd isotopic compositions are reported in Table A1 and Figure 4. There are significant variations in the Nd values of surface/subsurface seawater between stations. The most unradiogenic Nd isotopic composition of -6.7±0.3 is observed for the southernmost station SCS18-18 at surface depth (5 m) whereas the most radiogenic Nd value of -2.4±0.3 appears at a depth of 50 m at the northernmost station SCS18-25. For station SCS18-10, Nd values are -5.8±0.3 and -4.2±0.4 at depths of 20 m and 200 m, respectively.

Nd values of intermediate water range from -2.9±0.3 at a depth of 300 m to -3.9±0.3 at a depth of 1350 m at station SCS18-25. The Nd value of intermediate water at station SCS18-18 is slightly more negative (~-4.2) compared to stations SCS18-25 and SCS18-10 (~-3.7), with the exception of a less radiogenic value of -5.0±0.3 obtained at a depth of 1100 m at station SCS18-10. For the deep-water masses, Nd values for the three stations exhibit a narrow range from -3.4±0.3 to -4.2±0.3. Four seawater samples at station SDA3 display Nd values (from -3.7±0.3 to -4.3±0.3) that are similar to those found at corresponding depths at three other stations (from -3.5±0.3 to -4.2±0.3) (Figure 4).

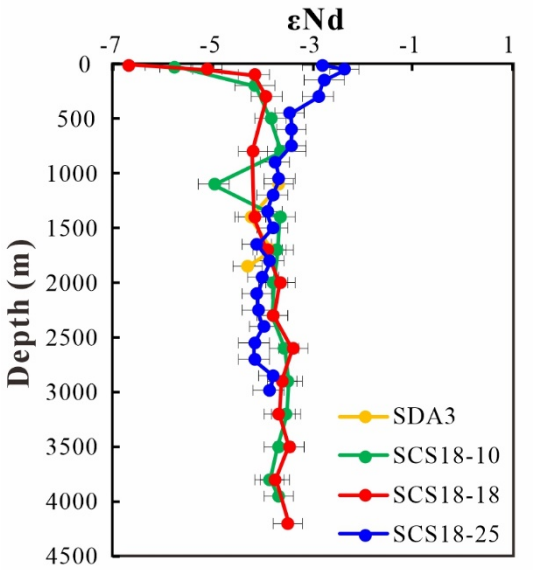

Figure 4. Vertical profiles of dissolved Nd isotopic composition investigated in this study.

4.3 Seawater REE concentrations and patterns

Overall, the REE concentrations increase with depth with the exception of Ce

concentrations which vary significantly at station SCS18-25. The vertical distributions of La, Nd and Yb concentrations have been plotted in Figure 5. The concentrations of La, Nd and Yb range from 8.48 to 45.55 pmol/kg, 8.46 to 27.51 pmol/kg and from 1.63 to 8.08 pmol/kg, respectively. Figure 5 shows that REE concentrations decrease slightly from surface to subsurface seawater with the exception of a minimum Nd concentration obtained at 5 m depth at station SCS18-10. The lowest concentrations of other REE were observed at 50 m depth at SCS18-18, 150 m depth at SCS18-25 and 200 m depth at SCS18-10. Below these water depths, REE concentrations obtained from stations SCS18-10 and SCS18-25 gradually increase with depth except for those of several bottom samples collected near the seafloor, from where they decrease slightly. Such a decrease is not observed at station SCS18-18 due to the lack of bottom water samples.

PAAS-normalized REE patterns have been reported in supplementary Figure S1. Typical seawater REE patterns with a negative Ce anomaly and an enrichment in HREE were observed for all seawater samples, which are similar to the findings of previous studies in the SCS and open West Pacific (Wu et al., 2015., Behrens et al., 2020). In most cases, the levels of HREE enrichment are more pronounced in the deep-water samples than in the surface water samples.

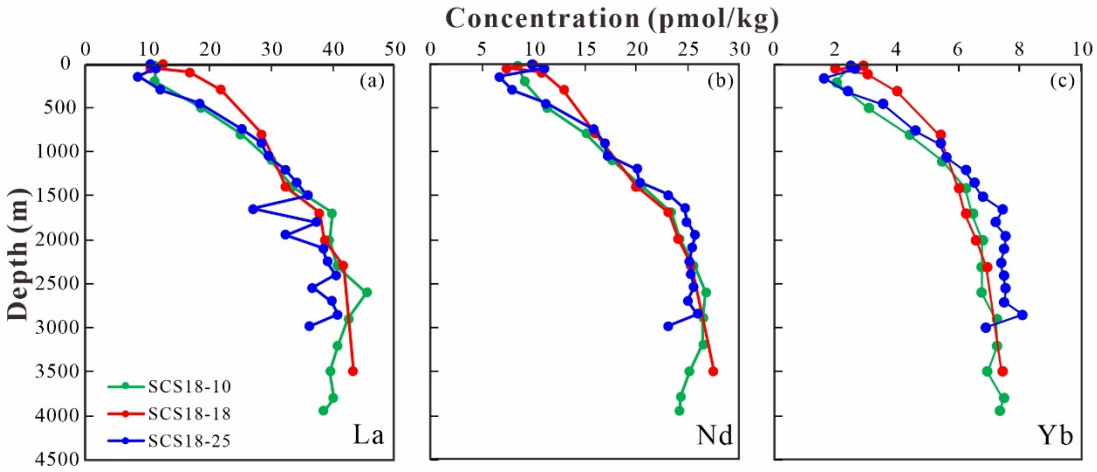

Figure 5. Vertical profiles of dissolved La (a), Nd (b), Yb (c) concentrations reported in this study.

5. Discussion

5.1 Continental sources to surface water of the SCS

In Figure 6, REE patterns of the SCS surface water have been reported together with previous results obtained for several stations in the SCS, the West Pacific and the eastern Indian Ocean (Alibo and Nozaki., 2000; Nozaki and Alibo., 2003; Wu et al., 2015; Brehens et al., 2018a). The linear plotted PAAS-normalized

REE patterns indicate that surface seawater REE concentrations in the SCS are generally higher than in the West Pacific but slightly lower than in the eastern Indian Ocean (Figure 6a). The SCS surface seawater is characterized by Nd concentrations between 8 and 15 pmol/kg, while in the West Pacific and the eastern Indian Ocean, Nd concentrations of surface seawater range from 2 to 8 pmol/kg, and from 18 to 51 pmol/kg, respectively. The significant increase in Nd concentration was also identified in previous studies carried out in the eastern Indian Ocean (Nozaki and Alibo., 2003; Yu et al., 2017; Hathorne et al., 2020). These investigations reveal that although a large quantity of REE was removed at mixing zones of fresh and salt water, the high REE concentrations of local surface seawater are associated with tremendous discharge from large Asian rivers such as the Ganges-Brahmaputra, Irrawaddy and Salween. Likewise, the SCS receives substantial sediment discharge from several large rivers characterized by high denudation rates induced by tectonic activity and heavy monsoon rainfall (Milliman and Farnsworth, 2011; Liu et al., 2016). Thus, the relatively high REE concentration of the SCS surface seawater can be attributed to particle dissolution induced by enhanced riverine inputs.

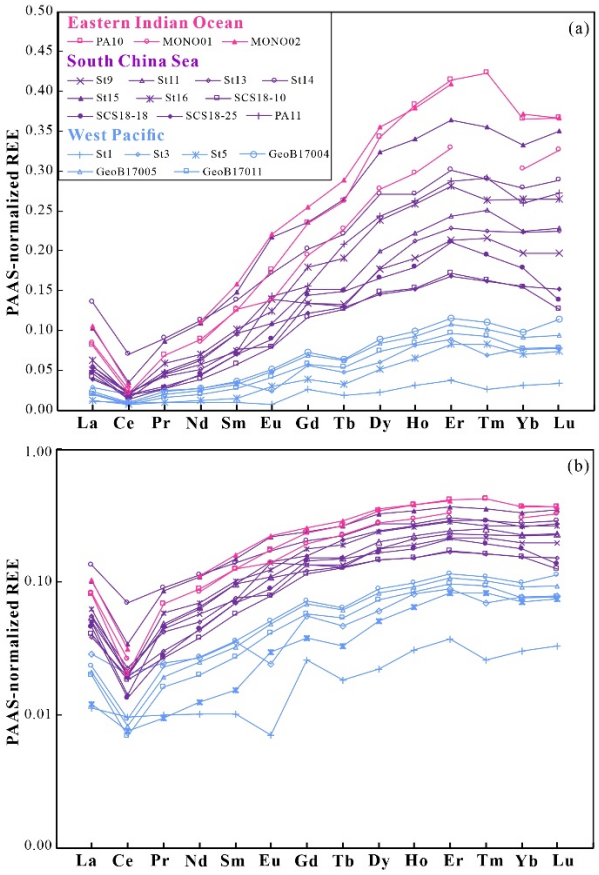

Figure 6. PAAS normalized REE patterns of surface seawater in the SCS, the West Pacific (Wu et al., 2015; Brehens et al., 2018a) and the eastern Indian Ocean (Nozaki and Alibo., 2003; Yu et al., 2017). The Fig. 6a and Fig. 6b are plotted with same data but in liner scale and log scales, respectively.

Similarly, the REE patterns of the SCS surface seawater, characterized by relatively MREE enrichment, in all likelihood, can be attributed to the influence of particulate dissolution related to substantial discharge from surrounding rivers.

PAAS-normalized REE patterns in a log-scale plot of surface seawater from all stations (including this study and literature data) exhibit relatively flat patterns with slight MREE enrichments (Figure 6b). These flat PAAS-normalized patterns were widely observed in surface seawater collected from different regions and especially from the marginal seas (Zheng et al., 2016; Yu et al., 2017). Many investigations into the REE of river water and submarine groundwater indicate that such MREE-enriched patterns are potentially carried by the colloidal phase, and are related to phosphate mineral weathering or iron hydroxide desorption (Hannigan and Sholkvitz, 2001., Tang and Johannesson, 2010; Hathorne et al., 2020). For example, it has previously been reported that Asian dusts play an important role in controlling the Nd isotopic compositions of surface sediments in the Philippine Sea (Jiang et al., 2013). This may indicate the effect of dust deposition on the MREE enrichment of surface seawater.

Despite limited data regarding REE in suspended particles in the SCS, there are several studies on the REE concentrations and patterns of filtered water, suspended particles and surface sediment of surrounding rivers (Chung et al., 2009; Bayon et al., 2015; Ma et al., 2019). These REE patterns together with surface seawater REE patterns of this study are shown in Figure 7. Both suspended river particles and river sediments display flat PAAS-normalized patterns. The REE patterns of the dissolved fraction of the Pearl River and Kaoping River exhibit apparent negative Ce anomalies and relative MREE enrichments (Figure 7). MREE enrichment of surface seawater in the SCS could be linked to particulate dissolution or the influence of river water discharge, which is consistent with the hydrographic parameter distribution characterized by fresher salinity in the surface layer (Tian et al., 2009; Xie et al., 2011).

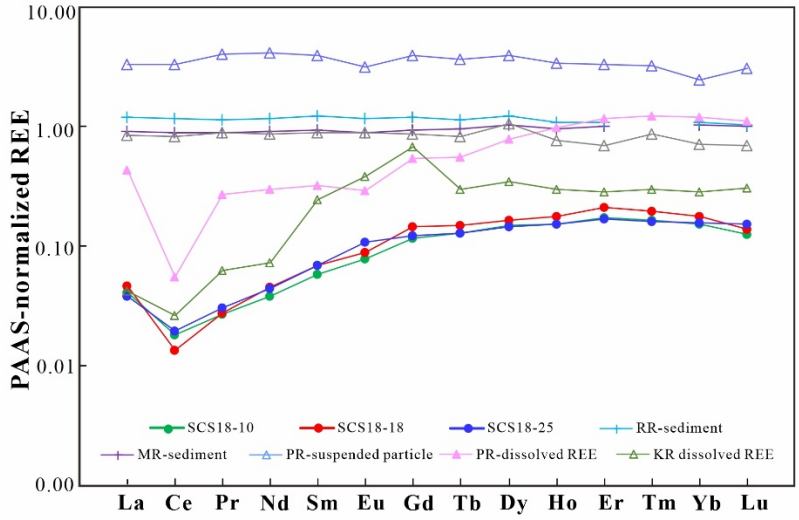

Figure 7. PAAS normalized REE patterns of surface seawater in the SCS ($*10^6$), Pearl River water (PR, *1) and Pearl River suspended particle (PR, $*10^{-3}$) (Ma et al., 2019), Kaoping River (KP) water (KP, $*10^2$) (Chung et a., 2009), Red River sediment (RR, $*10^{-3}$) and Mekong River sediment (MR, $*10^{-3}$) (Bayon et al., 2015).

In addition, an enhanced positive Gd anomaly, potentially related to anthropogenic waste disposal, has been extensively observed for a number of river water samples collected from Taiwan Island (Figure 7, Chung et al., 2009). Although such a strong positive Gd anomaly is not observed in the case of the SCS surface seawater, MREE enrichment in the SCS and the river water of Taiwan Island is similar.

5.2 Mechanisms controlling vertical distribution of REE in the SCS

5.2.1 Vertical distribution of REE in the SCS

Due to the dissolution of particles derived from various sources, such as dust and river sediment, the highest degree of MREE enrichment is generally found in the surface layer, apart from stations in the West Pacific where surface seawater is mainly occupied by NPTW with relatively low REE concentrations (Figure 8a, Wu et al., 2015; Brehens et al., 2018a). Consequently, the REE patterns of surface seawater of these stations are predominantly controlled by local inputs.

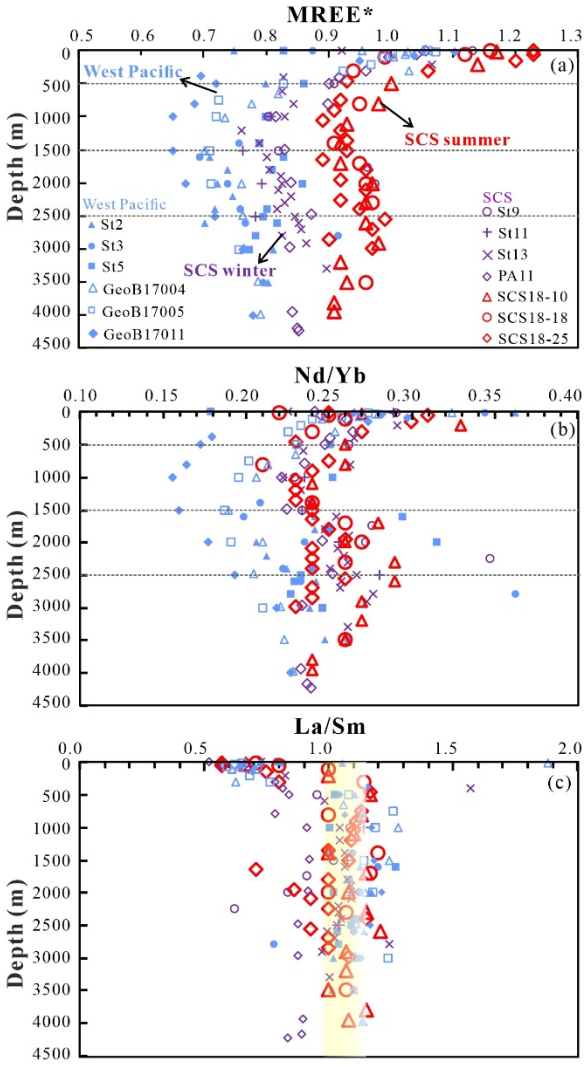

Figure 8. Vertical distribution of MREE*, Nd/Yb and La/Sm ratios in the SCS (this study and Wu et al., 2015) and in the West Pacific (Brehens et al., 2018a). MREE* are calculated using equation MREE*=2*(Sm+Eu+Gd+Dy)/(La+Ce+Nd+Ho+Er+Yb+Lu).

Previous studies show that water masses mixing and biogeochemical processes play an important role in controlling the vertical distribution of REE in the ocean (Garcia-Solsona et al., 2014; Molina-Kescher et al., 2014; Fr llje et al., 2016). The SCS is connected to the West Pacific, it is possible that the REE distribution in the SCS are also likely related to water masses intrusion and biogeochemical cycling. The plot of Nd concentration versus salinity (Figure 9) reveals distinguishable patterns between the surface water and the intermediate-

deep water. It shows that Nd concentration increases with increasing salinity for the surface seawater in the SCS, with the exception of the surface water at station SCS18-25 in the northernmost part of the SCS, which is generally influenced by the West Pacific. Nevertheless, Nd concentration vertical profiles of deep-water in the SCS display an increasing trend towards bottom water despite the relatively small variations in salinity due to the filling of homogenous PDW in the deep basin. In addition, representative REE values obtained from the SCS and the Philippine Sea are plotted versus the silicate concentrations at adjacent stations (Figure S2, Levitus et al., 2015). The results indicate a good correlation (R^2>0.8) between REE (especially the HREE, R^2>0.9) and silicate as shown in global ocean basins (Nozaki and Alibo, 2003; Akagi et al., 2011, 2013; Molina-Kescher et al., 2014).

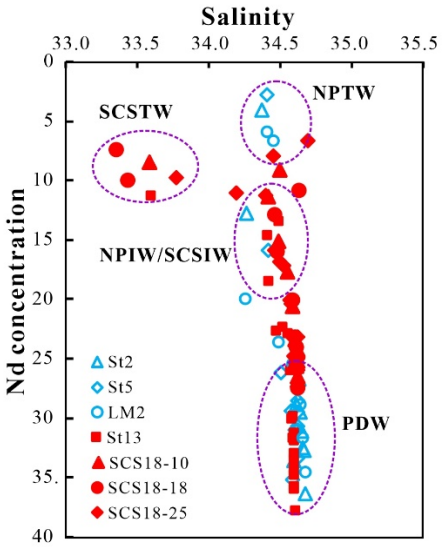

Figure 9. Nd concentration vs seawater salinity in the SCS (this study and Wu et al., 2015) and the North Pacific (Amakawa et al., 2004).

Since the deep-water in the SCS is predominantly influenced by the PDW from the West Pacific, normalizing deep-water SCS REE by NPDW's REE allows us to better constrain the sources and processes controlling REE distribution in the deep-basin of the SCS (Alibo and Nozaki., 2000). Figure 10 displays of the values for REE concentrations of the SCS at a depth of around 2500 m normalized to that conventionally used for the NPDW (Alibo and Nozaki., 1999). The MREE enrichments of the SCS deep water compared to the NPDW can be observed, which is consistent with the results of a previous study (Alibo and Nozaki., 2000). However, we do not observe the depletion of Gd, which is suggested to be caused by local terrigenous inputs by Alibo and Nozaki., (2000).

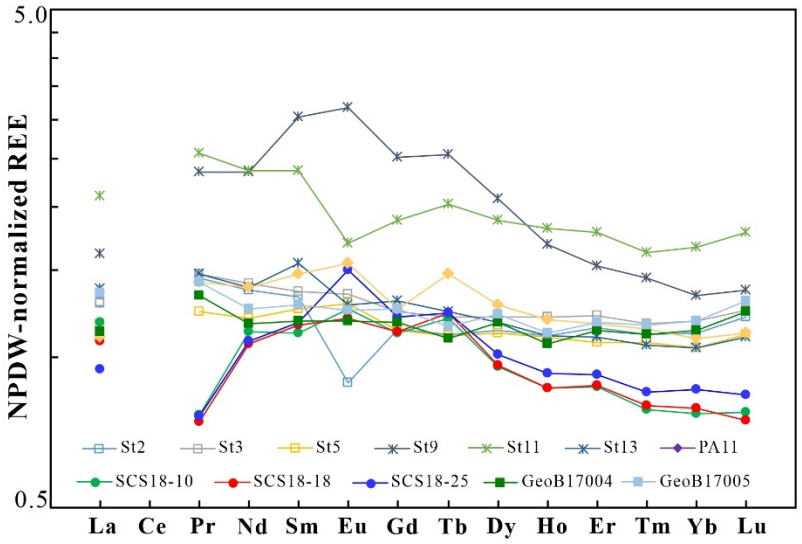

Figure 10. NPDW normalized REE patterns of deep water (~ 2500 m) from the SCS and the western Pacific Ocean. The published data for the SCS and the western Pacific Ocean are taken from Alibo and Nozaki., (2000), Wu et al., (2015), Brehens et al., (2018a). The NPDW concentration are taken from Alibo and Nozaki, (1999).

5.2.2 REE fractionation in the SCS

As discussed in 5.2.1, seawater REE-derived characteristics are most likely linked to water masses mixing and biogeochemical cycling in the SCS. To better understand how these fractionation processes control the REE patterns, comparisons of vertical profiles of PAAS-normalized MREE* values, La/Sm ratios and Nd/Yb ratios in this study and other studies over the region are presented (Figure 8, Alibo and Nozaki., 2000; Nozaki and Alibo, 2003; Wu et al., 2015; Brehens et al., 2018a).

The influence of water masses on REE fractionation were found in distinguished vertical MREE* variations between the SCS and the West Pacific (Figure 8a, Wu et al., 2015; Brehens et al., 2018a). Underlying the surface seawater, MREE enrichment is constantly less conspicuous in the West Pacific than in the SCS. The lowest MREE* values occurred at station of GeoB17011 located in the equatorial West Pacific (Figure 8a). The other stations in the Philippine Sea have relatively higher MREE* values compared to GeoB17011 but these values are still lower than those of the SCS stations. The highest MREE* values obtained at SCS stations were for seawater samples collected during the summer. In the study of REE and Nd isotope distributions in the West Pacific, the REE results for stations located in the Tropical West Pacific section indicate that the intermediate water is generally occupied by Antarctic Intermediate Water and differs from the NPIW at stations in the South Korea-open ocean

section (Brehens et al., 2018a, 2018b). The SCS intermediate water is mainly sourced from the NPIW and is vertically mixed with upwardly diffused deep water as indicated by the hydrographic properties. However, due to the regional seasonally reversed monsoon activity, the intrusion of the NPIW from the West Pacific also varies temporally (You et al., 2003; Tian et al., 2006; Yang et al., 2010). Thus, significant differences in the MREE* values for intermediate water between stations are likely to be linked to the variations in the locally predominant water masses.

The deep water in the SCS is homogenous and is mainly fed by the PDW from the West Pacific at a depth of about 2000 m (Tian et al., 2006). In this study, we find that below 1500 m, MREE* values increase continuously for water stations in the West Pacific. In the case of seawater samples collected from the SCS during the summer, MREE* values first increase and then decrease again from ~2500 m to the bottom water. In addition, MREE* values obtained from seawater collected in winter at SCS stations show a slight increase with depth whereas samples collected in summer are characterized by limited variations of MREE* values that are similar to those of intermediate water (Figure 8a). Hydrographical studies suggest that the deep water in the West Pacific is dominated by the Upper/Lower Circumpolar Deep Water (UCDW/LCDW) that originates from the Southern Ocean (Kawabe and Fujio., 2010). Regional REE investigations also indicate that REE distribution is largely controlled by lateral water mass transport and mixing (Brehens et al., 2018a, 2020). Consequently, the overall increased MREE* values of the West Pacific are probably linked to the almost identical deep-water mass deriving from southern-sourced (UCDW/LCDW). For the SCS, due to the limited sill depth of ~2000 m at the Luzon Strait, the effective water exchange between the SCS and the West Pacific mainly occurs above 2000 m (Qu et al., 2002, 2006; Tian et al., 2006; Wang et al., 2016, 2019).

Our study shows seasonal variations in MREE* distribution in the deep water of the SCS (Figure 8a). This is probably related to two phenomena: (1) the strong vertical mixing in the SCS (Tian et al., 2006; Sun et al., 2016; Wang et al., 2019), which results in limited variation between intermediate water and deep water; and (2) in winter, due to enhanced intrusion of deep water from the West Pacific and weaker deep water overflow to the West Pacific (Yang et al., 2010; Lan et al., 2015;). The higher proportion of fresh PDW means that the SCS's MREE* values are relatively similar to those of the West Pacific, as opposed to what is the case in the summer. This suggests that MREE* distribution in the intermediate and deep layer in the SCS is primarily controlled by water mass mixing.

Previous studies involving the partitioning of REE into various REE pools (e.g., truly dissolved fraction, labile particulate pool or iron oxides pool) demonstrate that LREE are more reactive to particles and are preferentially removed from seawater through the coagulation of the colloidal-associated REE fraction (de baar et al., 1985; Goldstein and Jacobsen., 1988; Byrne and Kim., 1990; Elder-

field et al., 1990). The REE fractionation in this study is might also related to this process. We observed that the MREE enrichment becomes weaker with increasing depths at stations of this study as well as other stations from the SCS and the West Pacific and the lowest MREE* values occurred at a depth of ~1500 in the West Pacific (Figure 8a). However, there is no distinction discernable between the La/Sm ratios of these stations (Figure 8c). On the other hand, the discrepancy in distributions of Nd/Yb ratios between stations is consistent with the distribution of MREE* values except that there is no visible difference in Nd/Yb ratios between the SCS stations (Figure 8a, b). Based on the comparable variation patterns between MREE* and Nd/Yb ratios, it is likely that MREE* variabilities in the different study areas are linked to spatial HREE variations. The downward decreasing MREE* values and Nd/Yb ratios in the SCS and the West Pacific are attributable to the extensive removal of LREE and MREE from the dissolved REE pool that generally results in the occurrence of HREE enrichment below surface seawater. This is further supported by decreasing MREE* values below 2500 m at three stations of this study (Figure 8a) that are probably related to comparatively greater scavenging of LREE and MREE by re-suspended sediments. Decreased bottom water REE concentrations have been observed in different ocean basins where they are attributed to REE scavenging by re-suspended particles from the seafloor (Alibo and Nozaki., 2000; Nozaki and Alibo., 2003; Singh et al., 2012; Molina-Kescher et al., 2014; Yu et al., 2017). Indeed, previous studies relying on multiple particle grain size and turbidity proxies have identified several benthic nepheloid layers in the northern SCS, caused by the occurrence of internal basin-scale waves (Chung et al., 2004; Zhang et al., 2014; Zhou et al., 2022). This is also supported by the variations in Nd/Yb and La/Sm ratios (Figure 8b, c), implying enhanced HREE enrichment compared to LREE and MREE for the water samples collected near the bottom.

Taken together, the vertical distribution of MREE* values, and La/Sm and Nd/Yb ratios indicate that the REE variations in the SCS are primarily controlled by water mass mixing and the particle scavenging process.

5.3 Distribution of Nd: particle-seawater reaction versus water mass source

5.3.1 The influence of particle dissolution on surface seawater Nd isotopic composition in the SCS

Surface seawater REE distributions in the northern SCS are significantly influenced by surrounding river sediment discharges. It has been reported elsewhere that these riverine inputs also fingerprint the Nd isotopic composition of the SCS surface seawater (Amakawa et al., 2000; Wu et al., 2015). A southward decrease in Nd is observed from the northern SCS to the central SCS. This spatial distribution pattern of surface seawater Nd isotopes agrees closely with previous studies illustrating that the most unradiogenic Nd isotopes are found in the southern SCS while the most radiogenic Nd isotopes occur in areas closest to Luzon Island in the north (Figure 11) (Amakawa et al., 2000; Wu et al.,

2015). This demonstrates that the surface seawater Nd isotopic compositions in the northern SCS are mostly affected by the advection of surface water masses from the NPTW, which is characterized by more radiogenic Nd signatures (-1.7±0.2~-3.1±0.2). However, away from the northern entrance of the Luzon Strait, surface seawater Nd isotopes in the SCS increasingly deviate from the characteristics of the original sourced water from the West Pacific and bear the fingerprint of the more negative Nd values of local river- and seafloor sediment (~-10, Liu et al., 2007; Wei et al., 2012). The potential influence of river particulates on seawater Nd isotopes has been described in different ocean margin areas (Jones et al., 1994; Singh et al., 2012; Haley et al., 2014; Yu et al., 2017). It has been suggested that suspended particles from river sediments or continental margins play a significant role in contributing to the global ocean Nd budget (Jones et al., 1994; Lacan et al., 2012; Rickli et al., 2014; Rousseau et al., 2015; Hathorne et al., 2020). The lithogenic particulate buried in near shore sediments might contain more labile colloid components and may release chemical elements into seawater as they are transported further away from estuary areas (Jones et al., 1994; Hathorne et al., 2020). In this case, our new Nd data for seawater obtained from the northern and central SCS support the hypothesis that the particle reaction induced by substantial sediment discharge plays an important role in controlling the surface seawater Nd as has been observed in many other marginal seas (Singh et al., 2012; Haley et al., 2014; Yu et al., 2017). This result indicates that the particle dissolution resulting from the riverine inputs not only has influences on surface seawater REE distribution but also on its Nd isotopic compositions in the SCS.

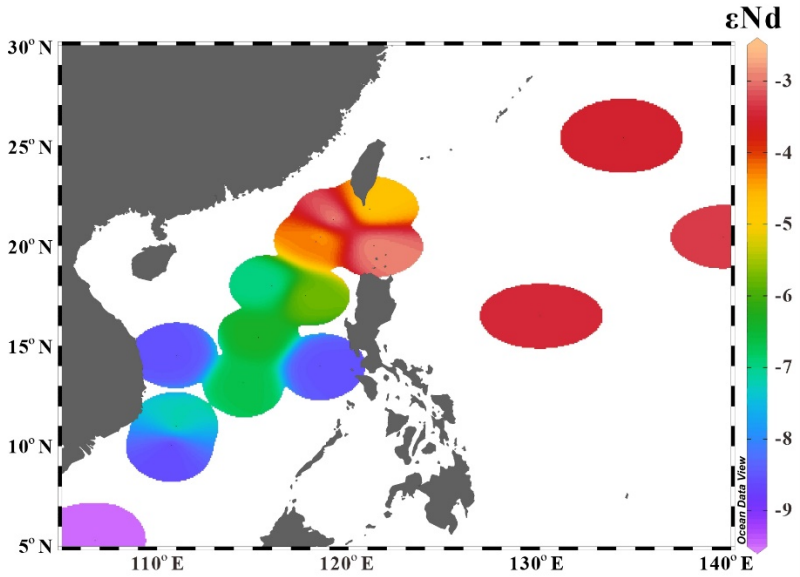

Figure 11. The distribution of Surface seawater Nd values in the SCS and the western Pacific Ocean. The reported Nd values are taken from Alibo and

Nozaki., (2000), Wu et al., (2015), Brehens et al., (2018a). The figure is plotted by ODV (Schlitzer, 2014).

5.3.2 Processes controlling Nd isotope distribution in intermediate and deep water in the SCS

The hydrographic properties and the REE distribution of the full water column in the SCS show that the intermediate and deep waters are mainly flushed from the Philippine Sea, accompanied by vertical diapycnal mixing within the SCS basin (Tian et al., 2009; Wang et al., 2019). Figure 4 reveals that the vertical variability of Nd signatures in the SCS is relatively small compared to the variabilities of REE concentrations. Nevertheless, we observed several excursions of Nd isotopic composition for water depths below the surface layers. A more exceptional negative Nd value of –5.0±0.3 was obtained at a depth of 1100 m for station SCS18-10 without any changes in the Nd concentration (Figure 4, 5). Previous studies have indicated that the main contributor of intermediate and deep circulation in the SCS is a mesoscale process (Zhang et al., 2013; Shu et al., 2019; Wang et al., 2019). The induction of this strong mesoscale eddy from upper layers to deeper layers potentially influences thousands of meters vertically and generates mid-deep ocean eddies in the SCS. Observation of particle deposition based on a mooring system shows that mesoscale eddies also play an important role in regulating vertical sediment transport in the deep SCS basin (Zhang et al., 2014). Station SCS18-10 is located in a region with enhanced sub-basin scale cyclonic currents around several seamounts (Wang et al., 2013). In addition, the transmissivity data for station SCS18-10 show a rapid decrease at a depth of around 1000 m indicating the existence of a nepheloid layer containing a large volume of suspended particulates (Figure S3). This suggests that the temporal negative excursion of seawater Nd values is probably related to particle-seawater exchanges that mainly impact seawater Nd isotopic composition without changing seawater Nd concentration. This is supported by experiments on the influence of particulate dissolution on seawater Nd values and REE concentrations, which found a rapid exchange of Nd values within 80 days between particles and seawater (Pearce et al., 2013).

In order to better constrain the behavior of Nd isotopes in the SCS and its relationship to the Nd signature in the West Pacific, Nd values of the SCS were compared to the northern and southern-sourced water masses of the Pacific Ocean. Figure 12a compares the representative vertical profiles of Nd isotopes for the SCS and the North Pacific (Piepgras and Jacobsen., 1988; Amakawa et al., 2004; Wu et al., 2015). Below 2000 m, Nd isotopes at each station in the SCS are generally within a small range of -3.4±0.3 to -4.2±0.3 compared to larger variations of Nd values in the North Pacific, with a more negative Nd value of -5.3±0.4 occurring at station LM2. Due to the modification caused by the input of surrounding volcanic material, the PDW/UCDW originating from the Southern Ocean were found to have similar Nd values of ~-4 in the western tropical Pacific Ocean (Amakawa et al., 2009; Grenier et al., 2013; Brehens et al., 2018a). Figure 12c shows that Nd values of deep-water in the SCS are also

comparable to deep water Nd values obtained from the western tropical Pacific Ocean. This indicates that the similarity in deep-water Nd values between the SCS and the West Pacific is probably due to a significant contribution of PDW/UCDW to the SCS deep-water and conservative behavior of Nd isotopes along the pathway of deep-water masses. In addition, different Nd signatures were observed between the bottom water of the SCS and its counterpart in the West Pacific. Due to the limited depth of the Luzon Strait (~2000 m), the overflow from the Philippine Sea to the SCS is primarily limited to within the upper 2000 m (Gong et al., 1992; Tian et al., 2006, 2009; Wang et al., 2019). Therefore, the homogenous Nd isotopic composition of bottom water in the SCS can be explained by a constant feed of PDW of ~2000 m from the West Pacific. Most of Nd signatures of bottom water in the SCS do not display modification despite the REE scavenging process induced by re-suspended particles. This suggests that the influence of re-suspended particles on seawater Nd isotopic composition by contributing additional REE sources to seawater is probably a local process that varies from site to site (Amakawa et al., 2004; Carter et al., 2012; Stichel et al., 2015).

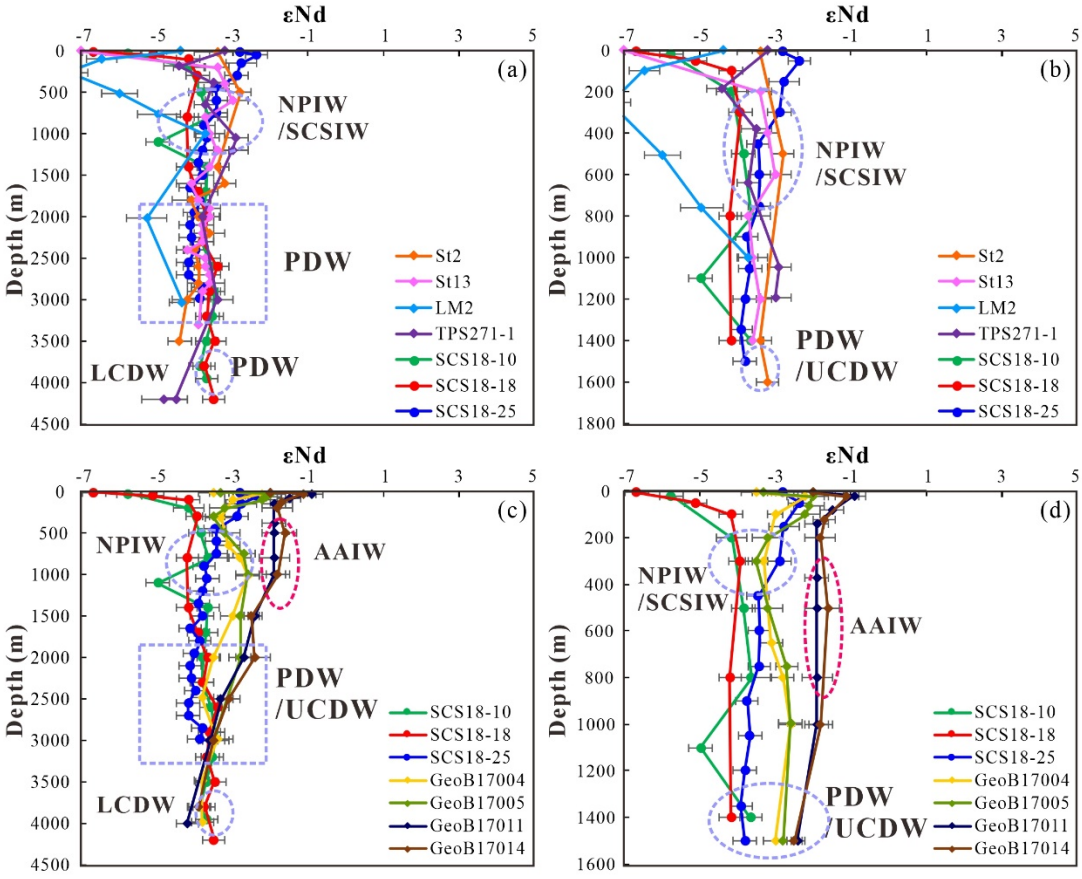

Figure 12. Vertical profiles of the full column and upper 1800 m showing the comparisons of Nd values between the SCS and the North Pacific (a, b) and between the SCS and the western Pacific Ocean (c, d). Nd values of the North Pacific and the western Pacific Ocean are taken from Piegras and Jacobsen, (1988), Amakawa et al., (2004), Wu et al., (2015), Brehens et al., (2018b).

Compared to deep water, Nd values of intermediate water in the SCS and the North Pacific are characterized by a relatively large range from -2.8±0.4 to -4.2±0.3 (Figure 12b). Figure 12b also shows that Nd isotopes of the SCSIW are slightly less radiogenic than those of the NPIW observed in the North Pacific. Additionally, the Nd values of SCS intermediate water are significantly lower than the Nd values (-1.6±0.3~-2.5±0.2) of intermediate water obtained from stations GeoB17011 (10.6342ºN, 148.9010ºE) and GeoB17014 (6.7842ºN, 154.1982ºE) located in the western tropical Pacific Ocean, (Figure 12d). It has been suggested that the intermediate water of these two stations (GeoB17014 and GeoB17011) consists mainly of southern-sourced AAIW which is characterized by less radiogenic Nd isotopes (Brehens et al., 2018b). Previous hydrographic observations have revealed that the northward propagated AAIW is mainly confined to the south of 13°N in the West Pacific (Qu et al., 1999; Qu and Lindstrom., 2004). The significant difference in Nd values between the SCSIW and the AAIW can be explained by the limited northward extension of AAIW so that it cannot reach the SCS through the Luzon Strait located further north of its pathway along the western boundary current. Thus, the main source of the intermediate water to the SCS is the NPIW that enters the SCS through the southern part of the Luzon Strait. Nevertheless, the SCSIW displays higher salinities than the NPIW due to the vertical diapycnal mixing in the SCS (Figure 2). The previous study also suggested that the relatively unradiogenic Nd isotopes of the SCSIW might be attributed to the additional input of more negative Nd from the deep water through vertical mixing of water masses (Wu et al., 2015). This is supported by the strong vertical supply of Nd from the subsurface layer to the surface layer, which is about two orders of magnitude greater than riverine/dust flux (Chen et al., 2013). Based on the global compilation of Nd data, Chen et al., 2013 argue that upper ocean supply of Nd to the ocean surface is an important factor controlling basin-scale surface seawater Nd budgets in less stratified regions. Vertical profiles of Nd concentration obtained from deep water of the South Pacific have revealed an offset from conservative mixing lines, which indicates that vertical cycling of Nd plays an important role in controlling regional Nd distribution (Molina-Kescher et al., 2014; Basak et al., 2015). Taking all reported Nd values for the SCSIW, we suggest that the vertical diapycnal mixing could potentially reduce stratification between the intermediate and deep waters in the SCS. Such water mass mixing probably leads to the supply of Nd from the deep water to the intermediate water in the SCS. Thus, in addition to the lateral transport of NPIW to the SCS, vertical cycling of Nd might also be a potential factor determining the Nd signature of the intermediate water.

Given all of the above, the present Nd isotopic composition of intermediate-

deep water in the SCS is globally consistent with that of its source NPIW and PDW, which indicates a relatively conservative Nd behavior along its pathway; it could therefore be used as a reliable proxy to trace water masses in regional paleoceanographic studies.

During the last glacial period when the sea level was low, it has been suggested that the deep water could be influenced by considerable sediment discharge to the SCS (Wu et al., 2017); the mechanism that controls the transfer of seawater Nd isotopes to sediment needs to be further investigated.

6. Conclusions

REE and Nd isotopes from four stations in the northern and central SCS are reported in this study. Our results permit a better understanding of the behavior of dissolved REE and Nd isotopes from the West Pacific to the northern, and the central SCS.

Our data reveals a general increase in REE concentration with depth, except for surface water and bottom water. The higher REE concentration of surface water in the SCS is linked to the significant sediment input from the surrounding large rivers, whereas the relatively low REE concentration of bottom water is attributable to the particle scavenging process.

The REE fractionation patterns, characterized by decreasing LREE and increasing HREE with depth in the SCS, linked to the particle scavenging process, are similar to the trends observed in the open ocean. Vertical profiles of MREE*, La/Sm and Nd/Yb indicate that the lateral transport of water mass from the West Pacific is the dominant factor governing REE distribution in the SCS. In addition, the good correlation between HREE enrichment and dissolved silicate contents implies that the distribution of HREE rather than LREE or MREE is related to biogeochemical cycling, consistent with the results of Akagi et al., (2011). The difference in the MREE* of intermediate water between the SCS and the West Pacific is attributable to cyclical vertical mixing within the SCS basin. The observed seasonal variation in REE patterns could be explained by a stronger intrusion of intermediate-deep water from the West Pacific and/or enhanced vertical water mass mixing in winter induced by regional monsoon activities.

Overall, the seawater Nd isotopic composition of the SCS reflects the advection of water masses, except for the surface water, with large spatial variations in Nd values. The more negative Nd values of surface water demonstrate the important role of substantial river sediment discharge in modifying the Nd isotopic composition of surface seawater, especially for the locations away from the entrance of surface seawater through the Luzon Strait.

The intermediate water Nd values are slightly more negative compared to corresponding NPIW in the West Pacific. The Nd signature of AAIW is not observed in the SCS as the route of the AAIW is generally confined to the south of 13^{o}N along the western boundary current. The relatively unradiogenic Nd isotope

values for intermediate water are most likely the result of vertical diapycnal mixing with deep water. The negative excursion of Nd values observed at a depth of ~1100 m is possibly related to a local nepheloid layer.

Nd isotopic composition of the deep water in the SCS is characterized by a homogenous value of ~-3.8±0.4. This is in good agreement with the values for the PDW at a depth of ~2000 m obtained in the West Pacific (Wu et al., 2015; Brehens et al., 2018b) and thus provides evidence for the conservative behavior of Nd isotopes during the propagation of deep water from the West Pacific to the SCS.

Acknowledgements

We thank the scientific team, the captain and crew of R/V Jiageng for their collaboration during sampling. We thank Jiawang Wu for his fruitful discussions. This research was supported by National Natural Science Foundation of China (Nos. 42176058, 42130407, and 41506057), Open Fund of the Key Laboratory of Marine Geology and Environment, Chinese Academy of Sciences (No. MGE2019KG12), and the Labex L-IPSL (n°ANR-10-LABX-0018).

Open Research

All the REE concentrations of this study are available online at the data publisher, PANGAEA (www.pangaea.de, https://doi.pangaea.de/10.1594/PANGAEA.943241).

References:

Abbott, A. N., Haley, B., McManus, J., & Reimers, C. (2015). The sedimentary source of dissolved rare earth elements to the ocean. *Geochimica et Cosmochimica Acta, 154*, 186-200. https://doi.org/10.1016/j.gca.2015.01.010

Abbott, A. N., Haley, B.A., & McManus, J. (2016). The impact of sedimentary coatings on the diagenetic Nd flux. *Earth and Planetary Science Letters, 449*, 217-227. https://doi.org/10.1016/j.epsl.2016.06.001

Akagi, T. (2013). Rare earth element (REE)–silicic acid complexes in seawater to explain the incorporation of REEs in opal and the "leftover" REEs in surface water: new interpretation of dissolved REE distribution profiles. *Geochimica et Cosmochimica Acta, 113*, 174-192. https://doi.org/10.1016/j.gca.2013.03.014

Akagi T., Fu F.-F., Hongo Y., & Takahashi K. (2011). Compositionof rare earth elements in settling particles collected in the highly productive North Pacific Ocean and Bering Sea: implications for siliceous-matter dissolution kinetics and formation of two REE-enriched phases. *Geochimica et Cosmochimica Acta, 75*, 4857-4876. https://doi.org/10.1016/j.gca.2011.06.001

Alibo, D. S., & Nozaki, Y. (1999). Rare earth elements in seawater: particle association, shale normalization, and Ce oxidation. *Geochimica et Cosmochimica Acta, 63*, 363-372. https://doi.org/10.1016/S0016-7037(98)00279-8

Alibo, D. S., & Nozaki, Y. (2000). Dissolved rare earth elements in the South China Sea: Geochemical characterization of the water masses, *Journal of Geophysical Research-Oceans, 105*, 28771-28783. https://doi.org/10.1029/1999JC000283

Amakawa, H., Alibo, D. S., & Nozaki Y. (2000). Nd isotopic composition and REE pattern in the surface waters of the eastern Indian Ocean and its adjacent seas. *Geochimica et Cosmochimica Acta, 64*, 1715-1727. https://doi.org/10.1016/S0016-7037(00)00333-1

Basak, C., Pahnke, K., Frank, M., Lamy, F., & Gersonde, R., (2015). Neodymium isotopic characterization of Ross Sea bottom water and its advection through the southern South Pacific. *Earth and Planetary Science Letters, 419*, 211-221. https://doi.org/10.1016/j.epsl.2015.03.011

Bayon, G., Toucanne, S., Skonieczny, C., André, L., Bermell, S., Cheron, S., et al. (2015). Rare earth elements and neodymium isotopes in world river sediments revisited, *Geochimica et Cosmochimica Acta, 170*, 17-38. https://doi.org/10.1016/j.gca.2015.08.001

Behrens, M. K., Pahnke, K., Paffrath, R., Schnetger, B., & Brumsack, H. J., (2018a). Rare earth element distributions in the West Pacific: trace element sources and conservative vs. non-conservative behavior. *Earth and Planetary Science Letters, 486*, 166-177. https://doi.org/10.1016/j.epsl.2018.01.016

Behrens, M. K., Pahnke, K., Schnetger, B., & Brumsack, H.-J. (2018b). Sources and processes affecting the distribution of dissolved Nd isotopes and concentrations in the West Pacific. *Geochimica et Cosmochimica Acta, 222*, 508-534. https://doi.org/10.1016/j.gca.2017.11.008

Behrens, M. K., Pahnke, K., Cravatte, S., Marin, F., & Jeandel, C. (2020). Rare earth element input and transport in the near-surface zonal current system of the Tropical Western Pacific. *Earth and Planetary Science Letters, 549*, 116496. https://doi.org/10.1016/j.epsl.2020.116496.

Broecker, W. S., Patzert, W. C., Toggweiler, J. R., & Stuive, M. (1986). Hydrography, chemistry, and radioisotopes in the southeast Asian basins, *Journal of Geophysical Research-Oceans, 91*, 14345-14354. https://doi.org/10.1029/JC091iC12p14345

Byrne, R. H., & Kim, K. H. (1990). Rare-earth element scavenging in seawater. *Geochimica et Cosmochimica Acta, 54*, 2645-2656. https://doi.org/10.1016/0016-7037(90)90002-3

Carter, P., Vance, D., Hillenbrand, C. D., Smith, J. A., & Shoosmith, D. R. (2012). The neodymium isotopic composition of waters masses in the eastern Pacific sector of the Southern Ocean. *Geochimica et Cosmochimica Acta, 79*, 41-59. https://doi.org/10.1016/j.gca.2011.11.034

Chen, G., Wang, D., Dong, C., Zu, T., Xue, H., Shu, Y., et al. (2015). Observed deep energetic eddies by seamount wake. *Scientific Reports, 5*:17416. https:

//doi.org/10.1038/srep17416

Chen, T., Stumpf, R., Frank, M., Beldowski, J., & Staubwasser, M. (2013). Contrasting geochemical cycling of hafnium and neodymium in the central Baltic Sea. *Geochimica et Cosmochimica Acta, 123*, 166-180. https://doi.org/10.1016/j.gca.2013.09.011

Chung, C.-H., You, C.-F., & Chu, H. -Y. (2009). Weathering sources in the Gaoping (Kaoping) river catchments, southwestern Taiwan: Insights from major elements, Sr isotopes, and rare earth elements. *Journal of Marine Systems, 76*, 433-443. https://doi.org/10.1016/j.jmarsys.2007.09.013

Chung, Y., Chang, H. C., & Hung. G. W. (2004). Particulate flux and ^{210}Pb determined on the sediment trap and core samples from the northern South China Sea, *Continental of Shelf Research, 24*, 673-691. https://doi.org/10.1016/j.csr.2004.01.003

Colin, C., Duhamel, M., Siani, G., Dubois-Dauphin, Q., Ducassou, E., Liu, Z., et al. (2021). Changes in the intermediate water masses of the Mediterranean Sea during the last climatic cycle - New constraints from neodymium isotopes in foraminifera, *Paleoceanography and Paleoclimatology, 36*(4). 1-28. https://doi.org/10.1029/2020PA004153

Colin, C., Tisnérat-Laborde, N., Mienis, F., Collart, T., Pons-Branchu, E., Dubois-Dauphin, Q., et al. (2019). Millennial-scale variations of the Holocene North Atlantic mid-depth gyre inferred from radiocarbon and neodymium isotopes in cold water corals. *Quaternary Science Reviews, 211*, 93-106. https://doi.org/10.1016/j.quascirev.2019.03.011

Copard, K., Colin, C., Douville, E., Freiwald, A., Gudmundsson, G., De Mol, B., & Frank, N. (2010). Nd isotopes in deep-sea corals in the North-eastern Atlantic. *Quaternary Science Reviews, 29* (19–20), 2499-2508. https://doi.org/10.1016/j.quascirev.2010.05.025

de Baar, H. J. W., Bacon, M. P., Brewer, P. G., & Bruland, K. W. (1985). Rare earth elements in the Atlantic and Pacific Oceans, *Geochimica et Cosmochimica Acta, 49*, 1943-1959. https://doi.org/10.1016/0016-7037(85)90089-4

de Baar, H. J. W., Bruland, K. W., Schijf, J., van Heuven, S. M. A. C., & Behrens, M. K. (2018). Low cerium among the dissolved rare earth elements in the central North Pacific Ocean, Geochimica et Cosmochimica Acta, 236, 5-40. https://doi.org/10.1016/j.gca.2018.03.003

Du, J., Haley, B. A., & Mix. A. C. (2020). Evolution of the Global Overturning Circulation since the Last Glacial Maximum based on marine authigenic neodymium isotopes. Quaternary Science Reviews, 241. 106396. https://doi.org/10.1016/j.quascirev.2020.106396.

Du, J., Haley, B.A., & Mix, A.C. (2016). Neodymium isotopes in authigenic phases, bottom waters and detrital sediments in the Gulf of Alaska and their

implications for paleocirculation reconstruction. *Geochimica et Cosmochimica Acta, 193*, 14-35. https://doi.org/10.1016/j.gca.2016.08.005

Dubois-Dauphin, Q., Bonneau, L., Colin, C., Montero-Serrano, J.-C., Montagna, P., Blamart, D., et al. (2016). South Atlantic intermediate water advances into the North-east Atlantic with reduced Atlantic meridional overturning circulation during the last glacial period. *Geochemistry, Geophysics, Geosystems, 17*, 2336-2353. https://doi.org/10.1002/2016GC006281

Elderfield, H. (1988). The oceanic chemistry of the rare-earth elements. *Philosophical Transactions of the Royal Society of London. Series A, Mathematical and Physical Sciences, 325*, 105-126. https://doi.org/10.1098/rsta.1988.0046

Elderfield, H., Upstillgoddard, R., & Sholkovitz E. R. (1990). The rare-earth elements in rivers, estuaries, and coastal seas and their significance to the composition of ocean waters. *Geochimica et Cosmochimica Acta, 54*, 971-991. https://doi.org/10.1016/0016-7037(90)90432-K

Fang, W., Guo, Z., & Huang, Y. (1998). Observational study of the circulation in the southern South China Sea, *Chinese Science Bulletin, 43*, 898-905. https://doi.org/10.1007/BF02884607

Fröllje, H., Pahnke, K., Schnetger, B., Brumsack, H.-J., Dulai, H., & Fitzsimmons, J.N., (2016). Hawaiian imprint on dissolved Nd and Ra isotopes and rare earth elements in the central North Pacific: local survey and seasonal variability. *Geochimica et Cosmochimica Acta, 189*, 110-131. https://doi.org/10.1016/j.gca.2016.06.001

Gan, J., Liu, Z., & Hui, R. (2016). A three-layer alternating spinning circulation in the South China Sea. *Journal of Physical Oceanography, 46*, 2309-2315. https://doi.org/10.1175/JPO-D-16-0044.1

Garcia-Solsona, E., Jeandel, C., Labatut, M., Lacan, F., Vance, D., Chavagnac, V., & Pradoux, C. (2014). Rare earth elements and Nd isotopes tracing water mass mixing and particle– seawater interactions in the SE Atlantic. *Geochimica et Cosmochimica Acta, 125*, 351-372. https://doi.org/10.1016/j.gca.2013.10.009

Goldstein, S. J., & Jacobsen, S. B. (1988). Rare earth elements in river waters, *Earth and Planetary Science Letters, 89*, 35-47. https://doi.org/10.1016/0012-821X(88)90031-3

Gong, G.-C., Liu, K. K., Liu, C.-T., & Pai, S.-C. (1992). The Chemical Hydrography of the South China Sea West of Luzon and a Comparison with the West Philippine Sea. *Terrestrial, Atmospheric and Oceanic Sciences Journal, 3*, 587-602. https://doi.org/10.3319/TAO.1992.3.4.587(O)

Grasse, P., Bosse, L., Hathorne, E. C., Böning, P., Pahnke, K., & Frank, M. (2017). Short-term variability of dissolved rare earth elements and neodymium isotopes in the entire water column of the Panama Basin. *Earth and Planetary Science Letters, 475*, 242-253. https://doi.org/10.1016/j.epsl.2017.07.022

Greaves, M. J., Statham, P. J., & Elderfield, H. (1994). Rare earth element mobilization from marine atmospheric dust into seawater. *Marine Chemistry, 46*, 255-260. https://doi.org/10.1016/0304-4203(94)90081-7

Grenier, M., Jeandel, C., Lacan, F., Vance, D., Venchiarutti, C., Cros, A., & Cravatte, S. (2013). From the subtropics to the central equatorial Pacific Ocean: neodymium isotopic composition and rare earth element concentration variations. *Journal of Geophysical Research-Oceans, 118*, 592-618. https://doi.org/10.1029/2012JC008239

Haley, B. A., Frank, M., Hathorne, E., & Pisias, N. (2014). Biogeochemical implications from dissolved rare earth element and Nd isotope distributions in the Gulf of Alaska. *Geochimica et Cosmochimica Acta, 126*, 455-474. https://doi.org/10.1016/j.gca.2013.11.012

Haley, B. A., Du, J., Abbott, A. N., & McManus, J. (2017). The Impact of Benthic Processes on Rare Earth Element and Neodymium Isotope Distributions in the Oceans. *Frontier in Marine Science, 4*, 426. https://doi.org/10.3389/fmars.2017.00426.

Hannigan, R. E., & Sholkovitz, E. R. (2000). The development of middle rare earth element enrichments in freshwaters: weathering of phosphate minerals. *Chemical Geology, 175*, 495-508. https://doi.org/10.1016/S0009-2541(00)00355-7

Hathorne, E. C., Frank, M., & Mohan, P. M. (2020). Rare Earth Elements in Andaman Island Surface Seawater: Geochemical Tracers for the Monsoon? Frontier in Marine Science, 6, 767. https://doi.org/10.3389/fmars.2019.00767.

Hu, J., Kawamura, H., Hong, H., & Qi, Y. (2000). A review on the currents in the South China Sea: Seasonal circulation, South China Sea warm current and Kuroshio intrusion. *Journal of Oceanography, 56*, 607-624. https://doi.org/10.1023/A:1011117531252

Jiang, F., Frank, M., Li, T., Chen, T., Xu, Z., & Li, A. (2013), Asian dust input in the western Philippine Sea: Evidence from radiogenic Sr and Nd isotopes, *Geochemistry, Geophysics, Geosystems, 14*, 1538–1551. https://doi.org/10.1002/ggge.20116

Johannesson, K., & Burdige, D. (2007). Balancing the global oceanic neodymium budget: evaluating the role of groundwater. *Earth and Planetary Science Letters, 253* (1-2), 129-142. https://doi.org/10.1016/j.epsl.2006.10.021

Jones, C. E., Halliday, A. N., Rea, D. K., & Owen, R. M. (1994). Neodymium isotopic variations in North Pacific modern silicate sediment and the insignificance of detrital REE contributions to seawater. E*arth and Planetary Science Letters,127*, 55-66. https://doi.org/10.1016/0012-821X(94)90197-X

Kawabe. M & Fujio. S. (2010). Pacific Ocean Circulation Based on Observation. *Journal of Oceanography, 66*, 389-403. https://doi.org/10.1007/s10872-010-0034-8

Kim, I., & Kim, G. (2014). Submarine groundwater discharge as a main source of rare earth elements in coastal waters. *Marine Chemistry, 160*, 11-17. https://doi.org/10.1016/j.marchem.2014.01.003

Lacan, F., & Jeandel, C. (2005). Neodymium isotopes as a new tool for quantifying exchange fluxes at the continent-ocean interface. *Earth and Planetary Science Letters, 232*, 245-257. https://doi.org/10.1016/j.epsl.2005.01.004

Lacan, F., Tachikawa, K., & Jeandel, C. (2012). Neodymium isotopic composition of the oceans: a compilation of seawater data. *Chemical Geology, 300*, 177-184. https://doi.org/10.1016/j.chemgeo.2012.01.019

Le Houedec, S., Meynadier, L., & Allègre, C. J. (2016). Seawater Nd isotope variation in the Western Pacific Ocean since 80 Ma (ODP 807, Ontong Java Plateau). *Marine Geology, 380*, 138-147. https://doi.org/10.1016/j.margeo.2016.07.005

Levitus, S., Boyer, T. P., Garcia, H. E., Locarnini, R. A., Zweng, M. M., Mishonov, A.V. et al. (2015). World Ocean Atlas 2013 (NCEI Accession 0114815). *NOAA National Centers for Environmental Information*. Dataset. https://doi.org/10.7289/v5f769gt.

Li, L., & Qu, T. (2006). Thermohaline circulation in the deep South China Sea basin inferred from oxygen distributions. *Journal of Geophysical Research-Oceans, 111*, https://doi.org/10.1029/2005JC003164.

Liu, Z., Colin, C., Huang, W., Le, K., Tong, S., Chen, Z., & Trentesaux, A. (2007). Climatic and tectonic controls on weathering in South China and the Indochina Peninsula: clay mineralogical and geochemical investigations from the Pearl, Red, and Mekong drainage basins. *Geochemistry, Geophysics, Geosystems, 8*, http://dx.doi.org/10.1029/2006GC001490.

Liu, Z., Zhao, Y., Colin, C., Stattegger, K., Wiesner, M. G., Huh, C.-A., et al. (2016). Source-to-sink transport processes of fluvial sediments in the South China Sea. *Earth-Science Reviews, 153*, 238-273. https://doi.org/10.1016/j.earscirev.2015.08.005

Lüdmann, T., Wong, H. K., & Berglar, K. (2005). Upward flow of North Pacific Deep Water in the northern South China Sea as deduced from the occurrence of drift sediments. *Geophysical Research Letters, 32*, https://doi.org/10.1029/2004GL021967.

Ma, L., Dang, D., Wang, W., Evans, R. D., & Wang. W. -X. (2019). Rare earth elements in the Pearl River Delta of China: Potential impacts of the REE industry on water, suspended particles and oysters. *Environmental Pollution, 244*, 190-201. https://doi.org/10.1016/j.envpol.2018.10.015

Lan, J., Wang, Y., Cui, F., & Zhang, N. (2015). Seasonal variation in the South China Sea deep circulation. *Journal of Geophysical Research-Oceans, 120*, 1682-1690. https://doi.org/10.1002/2014JC010413

Milliman, J. D., & Farnsworth, K. L., (2011). River Discharge to the Coastal Ocean: A Global Synthesis. *Cambridge University Press, Cambridge* (pp. 384).

Molina-Kescher, M., Frank, M., & Hathorne, E. (2014). South Pacific dissolved Nd isotope compositions and rare earth element distributions: water mass mixing versus biogeochemical cycling. *Geochimica et Cosmochimica Acta, 127*, 171-189. https://doi.org/10.1016/j.gca.2013.11.038

Molina-Kescher, M., Frank, M., Tapia, R., Ronge, T. A., Dirk Nürnberg, D., & Tiedemann, R. (2016). Reduced admixture of North Atlantic Deep Water to the deep central South Pacific during the last two glacial periods. *Paleoceanography and Paleoclimatology, 31*, 651-668. https://doi.org/10.1002/2015PA002863

Noble, T. L., Piotrowski, A. M., & McCave, I. N. (2013). Neodymium isotopic composition of intermediate and deep waters in the glacial southwest Pacific. *Earth and Planetary Science Letters, 384*, 27-36. https://doi.org/10.1016/j.epsl.2013.10.010

Nozaki, Y., & Alibo, D.S. (2003). Importance of vertical geochemical processes in controlling the oceanic profiles of dissolved rare earth elements in the northeastern Indian Ocean. *Earth and Planetary Science Letters, 205*, 155-172. https://doi.org/10.1016/S0012-821X(02)01027-0

Osborne, A. H., Haley, B. A., Hathorne, E. C., Flögel, S., & Frank, M. (2014). Neodymium isotopes and concentrations in Caribbean seawater: tracing water mass mixing and continental input in a semi-enclosed ocean basin. *Earth and Planetary Science Letters, 406*, 174-186. https://doi.org/10.1016/j.epsl.2014.09.011

Pearce, C. R., Jones, M. T., Oelkers, E. H., Pradoux, C., & Jeandel, C. (2013). The effect of particulate dissolution on the neodymium (Nd) isotope and rare earth element (REE) composition of seawater. *Earth and Planetary Science Letters, 369*, 138-147. https://doi.org/10.1016/j.epsl.2013.03.023

Piepgras, D. J, & Jacobsen, S. B. (1988). The isotopic composition of neodymium in the North Pacific. *Geochimica et Cosmochimica Acta, 52*, 1373-1381. https://doi.org/10.1016/0016-7037(88)90208-6

Piotrowski, A. M., Goldstein, S. L., Hemming, S. R., & Fairbanks, R. G. (2005). Temporal relationships of carbon cycling and ocean circulation at glacial boundaries. *Science, 307*,1933-1938. https://doi.org/10.1126/science.1104883

Piotrowski, A. M., Galy, A., Nicholl, J. A. L., Roberts, N., Wilson, D. J., Clegg, J. A., & Yu, J. (2012). Reconstructing deglacial North and South Atlantic deep water sourcing using foraminiferal Nd isotopes. *Earth and Planetary Science Letters, 357-358*, 289-297. https://doi.org/10.1016/j.epsl.2012.09.036

Qu, T. (1999). Upper layer circulation in the South China Sea, *Journal of Physical Oceanography, 30*, 1450-1460. https://doi.org/10.1175/1520-0485(2000)030%3c1450:ULCITS%3e2.0.CO;2

Qu, T. (2002), Evidence of water exchange between the South China Sea and the Pacific through the Luzon Strait, *Acta Oceanologica Sinica, 21*, 175– 185.

Qu, T., Girton, J. B., & Whitehead, J. A. (2006). Deepwater overflow through Luzon Strait. *Journal of Geophysical Research-Oceans, 111*, https://doi.org/10.1029/2005JC003139.

Qu, T., & Lindstrom, E. (2004), Northward intrusion of Antarctic Intermediate Water in the western North Pacific, *Journal of Physical Oceanography, 34*, 2104-2118. https://doi.org/10.1175/1520-0485(2004)034%3c2104:NIOAIW%3e2.0.CO;2

Rickli, J., Gutjahr, M., Vance, D., Fischer-Gödde, M., Hillenbrand, C.-D., & Kuhn, G. (2014). Neodymium and hafnium boundary contributions to seawater along the West Antarctic continental margin. *Earth and Planetary Science Letters, 394*, 99-110. https://doi.org/10.1016/j.epsl.2014.03.008

Rousseau, T. C. C., Sonke, J. E., Chmeleff, J., Van Beek, P., Souhaut, M., Boaventura, G., Seyler, P., & Jeandel, C. (2015). Rapid neodymium release to marine waters from lithogenic sediments in the Amazon estuary. *Nature Communications, 6*, https://doi.org/10.1038/ncomms8592.

Scher, H., Whittaker, J., William, S., Latimer, J., Kordesch, W., & Delaney, M. (2015). On-set of Antarctic circumpolar current 30 million years ago as Tasmanian Gateway aligned with westerlies. *Nature, 523*, 580–583. https://doi.org/10.1038/nature14598

Schlitzer, R. (2014). Ocean data view. http://odv.awi.de.

Shu, Y., Xue, H., Wang, D., Chai, F., Xie, Q., Yao, J. L., & Xiao, J. G. (2014). Meridional overturning circulation in the South China Sea envisioned from the high-resolution global reanalysis data GLBa0.08. *Journal of Geophysical Research-Oceans, 119*, 3012-3028. https://doi.org/10.1002/2013JC009583

Shu, Y., Chen, J., Li, S., Wang, Q., Yu, J., & Wang, D. (2019). Field-observation for an anticyclonic mesoscale eddy consisted of twelve gliders and sixty-two expendable probes in the northern South China Sea during summer 2017. *Science China Earth Sciences, 62*, 451-458. https://doi.org/10.1007/s11430-018-9239-0

Singh, S. P., Singh, S. K., Goswami, V., Bhushan, R., & Rai, V. K. (2012). Spatial distribution of dissolved neodymium and eNd in the Bay of Bengal: role of particulate matter and mixing of water masses. *Geochimica et Cosmochimica Acta, 94*, 38-56. https://doi.org/10.1016/j.gca.2012.07.017

Stiche, T., Hartman, A. E., Duggan, B., Goldstein, S. L., Scher, H., & Pahnke, K. (2015) Separating biogeochemical cycling of neodymium from water mass mixing in the eastern North Atlantic. *Earth and Planetary Science Letters, 412*, 245-260. https://doi.org/10.1016/j.epsl.2014.12.008

Sun, H., Yang, Q., Zhao, W., Liang, X., & Tian, J. (2016). Temporal variability

of diapycnal mixing in the northern South China Sea. *Journal of Geophysical Research-Oceans, 121*, 8840-8848. https://doi.org/10.1002/2016JC012044

Tachikawa, K., Arsouze, T., Bayon, G., Bory, A., Colin, C., Dutay, J.- C., et al. (2017). The large-scale evolution of neodymium isotopic composition in the global modern and Holocene ocean revealed from seawater and archive data. *Chemical Geology, 457*, 131-148. https://doi.org/10.1016/j.chemgeo.2017.03.018

Tanaka, T., Togashi, S., Kamioka, H., Amakawa, H., Kagami, H., Hamamoto, T., et al. (2000). JNdi-1: A neodymium isotopic reference in consistency with LaJolla neodymium. *Chemical, Geology,* 168, 279-281. https://doi.org/10.1016/S0009-2541(00)00198-4

Tang, J., & Johannesson, K. H. (2010). Ligand extraction of rare earth elements from aquifer sediments: implications for rare earth element complexation with organic matter in natural waters. *Geochimica et Cosmochimica Acta, 74*, 6690-6705. https://doi.org/10.1016/j.gca.2010.08.028

Tian, J., Yang, Q., Liang, X., Xie, L., Hu, D., Wang, F., & Qu, T. (2006). Observation of Luzon Strait transport. *Geophysical Research Letters, 33*, https://doi.org/10.1029/2006GL026272.

Tian, J., Yang, Q., & Zhao, W. (2009). Enhanced diapycnal mixing in the South China Sea. *Journal of Physical Oceanography, 39*, 3191-3203. https://doi.org/10.1175/2009JPO3899.1

van de Flierdt, T., Griffiths, A.M., Lambelet, M., Little, S.H., Stichel, T., & Wilson, D.J. (2016). Neodymium in the oceans: a global database, a regional comparison and implications for palaeoceanographic research. *Philosophical transactions. Series A, Mathematical, Physical, and Engineering Sciences, 374*, 20150293. https://doi.org/10.1098/rsta.2015.0293.

Wang, D., Wang, Q., Zhou, W., Cai, S., Li, L., & Hong, B. (2013). An analysis of the current deflection around Dongsha Islands in the northern South China Sea. *Journal of Geophysical Research-Oceans, 118*, 490–501. https://doi.org/10.1029/2012JC008429

Wang, D., Wang, Q., Cai, S., Shang, X., Peng, S., Shu, Y., et al. (2019). Advances in research of the mid-deep South China Sea circulation. *Science China Earth Sciences, 62*, https://doi.org/10.1007/s11430- 019-9546-3.

Wang, D., Xiao, J., Shu, Y., Xie, Q., Chen, J., & Wang, Q. (2016). Progress on deep circulation and meridional overturning circulation in the South China Sea. *Science China Earth Science, 59*, 1827-1833. https://doi.org/10.1007/s11430-016-5324-6

Wang, G., Xie, S., Qu, T., & Huang, R. (2011). Deep South China Sea circulation. G*eophysical Research Letters, 38*, https://doi.org/10.1029/2010GL046626.

Wang, J., Shu, Y., Wang, D., Xie, Q., Wang, Q., Chen, J., et al. (2021).

Observed variability of bottom-trapped topographic Rossby Waves along the slope of the northern South China Sea. *Journal of Geophysical Research-Oceans, 126*, https://doi.org/10.1029/2021JC017746.

Wei, G., Liu, Y., Ma, J., Xie, L., Chen, J., Deng, W., &Tang, S. (2012). Nd, Sr isotopes and elemental geochemistry of surface sediments from the South China Sea: implications for provenance tracing. *Marine Geology, 319–322*, 21-34. https://doi.org/10.1016/j.margeo.2012.05.007

Wu, J., Pahnke, K., Böning, P., Wu, L., Michard, A., & de Lange, G.J. (2019). Divergent Mediterranean seawater circulation during Holocene sapropel formation – Reconstructed using Nd isotopes in fish debris and foraminifera. *Earth and Planetary Science Letters, 511*, 141-153. https://doi.org/10.1016/j.epsl.2019.01.036

Wu, Q., Colin, C., Liu, Z., Bassinot, F., Dubois-Dauphin, Q., Douville, E., Thil, F., & Siani., G. (2017). Foraminiferal Nd in the deep north-western subtropical Pacific Ocean: Tracing changes in weathering input over the last 30,000 years. *Chemical Geology, 470*, 55-66. https://doi.org/10.1016/j.chemgeo.2017.08.022

Wu, Q., Colin, C., Liu, Z., Douville, E., Dubois-Dauphin, Q., & Frank, N. (2015). New insights into hydrological exchange between the South China Sea and the Western Pacific Ocean based on the Nd isotopic composition of seawater. *Deep-Sea Research II, 122*, 25-40. https://doi.org/10.1016/j.dsr2.2015.11.005

Xie, L., Tian, J., Zhang, S., Zhang, Y., & Yang., Q. (2011). An anticyclonic eddy in the intermediate layer of the Luzon Strait in Autumn 2005. *Journal of Oceanography, 67*, 37-46. https://doi.org/10.1007/s10872-011-0004-9

Yang, Q., Tian, J., & Zhao, W. (2010). Observation of Luzon Strait transport in summer 2007. *Deep-Sea Research Part I, 57*, 670-676. https://doi.org/10.1016/j.dsr.2010.02.004

You, Y. (2003). The pathway and circulation of North Pacific Intermediate Water, *Geophysical Research Letters, 30*, 2291, https://doi:10.1029/2003GL018561.

Yu, Z., Colin, C., Douville, E., Meynadier, L., Duchamp-Alphonse, S., Sepulcre, S., et al. (2017a). Yttrium and rare earth element partitioning in seawaters from the Bay of Bengal. *Geochemistry, Geophysics, Geosystems, 18*, 1388-1403. https://doi.org/10.1002/2016GC006749

Yuan, D. (2002). A numerical study of the South China Sea deep circulation and its relation to the Luzon Strait transport. *Acta Oceanologica Sinica, 21*, 187-202.

Zhang, X., Huang, X., Zhang, Z., Zhou, C., Tian, J., & Zhao, W. (2018). Polarity variations of internal solitary waves over the continental shelf of the northern South China Sea: Impacts of seasonal stratification, mesoscale eddies, and internal tides. *Journal of Physical Oceanography, 48*, 1349-1365. https://doi.org/10.1175/JPO-D-17-0069.1

Zhang, Y., Liu, Z, Zhao, Y., Wang, W. G., Li, J. R., & Xu, J. P. (2014). Mesoscale eddies transport deep-sea sediments. *Scientific Reports, 4*, https://doi.org/10.1038/srep05937.

Zhang, Z., Zhao, W., Tian, J., & Liang, X. (2013). A mesoscale eddy pair southwest of Taiwan and its influence on deep circulation. *Journal of Geophysical Research-Oceans, 118*, 6479-6494. https://doi.org/10.1002/2013JC008994

Zheng, X, Plancherel, Y., Saito, M. A., Scott, P. M., & Henderson, G. M., (2016). Rare Earth elements (REEs) in the tropical South Atlantic and quantitative deconvolution of their non-conservative behavior. *Geochimica et Cosmochimica Acta, 177*, 217–237. https://doi.org/10.1016/j.gca.2016.01.018

Zhou, C., Zhao, W., Tian, J., Zhao, X., Zhu, Y., Yang, Q., & Qu, T. (2017). Deep western boundary current in the south china sea. *Scientific Reports, 7*, https://doi.org/10.1038/s41598-017-09436-2.

Zhou, M., Wang, G., Liu, W., & Chen, C. (2020). Variability of the observed deep western boundary current in the South China Sea. *Journal of Physical Oceanography, 50*, 2953-2963. https://doi.org/10.1175/JPO-D-20-0013.1

Zhu, Y., Fang, G., Wei, Z., Wang, Y., Teng, F., & Qu, T. (2016). Seasonal variability of the meridional overturning circulation in the South China Sea and its connection with inter-ocean transport based on SODA2.2.4. *Journal of Geophysical Research-Oceans, 121*, 3090–3105. https://doi.org/10.1002/2015JC011443

Zhou, W., Cao, W., Zhao, J., Wang, G., Zheng, W., Deng, L., & Cai Li, (2022). Variability of scattering and backscattering of marine particles in relation to particle concentration, size distribution, and composition off the eastern hainan coast in the south China sea, *Continental Shelf Research, 232*, 104615, https://doi.org/10.1016/j.csr.2021.104615.

Zhu, Y., Sun, J., Wang, Y., Wei, Z., Yang, D., & Qu, T. (2017). Effect of potential vorticity flux on the circulation in the South China Sea. *Journal of Geophysical Research-Oceans, 122*, 6454-6469. https://doi.org/10.1002/2016JC012375

Zhu, Y., Sun, J., Wang, Y., Li, S., Xu, T., Wei, Z., & Qu, T. (2019). Overview of the multi-layer circulation in the South China Sea. *Progress in Oceanography, 175*, 171-182. https://doi.org/10.1016/j.pocean.2019.04.001